# Synthesis of Ti matrix composites reinforced with TiC particles: in situ synchrotron X-ray diffraction and modeling

Jérôme Andrieux, Bruno Gardiola, Olivier Dezellus

To cite this paper : *J. Andrieux, B. Gardiola, O. Dezellus, Synthesis of Ti matrix composites reinforced with TiC particles: in-situ synchrotron X ray diffraction and modeling, Journal of Materials Science 2018, Accepted for publication, doi 10.1007/s10853-018-2258-8.*

# Synthesis of Ti matrix composites reinforced with TiC particles: in-situ synchrotron X-ray diffraction and modeling.

Jérôme Andrieux *, Bruno Gardiola, Olivier Dezellus

Université Claude Bernard Lyon 1, CNRS, Laboratoire des Multimatériaux et Interfaces, F-69622 Villeurbanne, France.

* Corresponding author: Jérôme Andrieux

Laboratoire des Multimatériaux et Interfaces – UMR CNRS 5615,

Université Claude Bernard Lyon 1,

43 Bd du 11 novembre 1918,

Villeurbanne, 69100, France

Tel: +334.72.44.80.79. Fax: +334.72.44.06.18.

e-mail: jerome.andrieux@univ-lyon1.fr

**Abstract**

The reaction tending towards thermodynamic equilibrium during the synthesis of Ti/TiC MMC prepared by the powder metallurgy route was studied by in-situ synchrotron X-ray diffraction. The carbide composition was found to change rapidly from its initial stoichiometric value $TiC_{0.96}$ towards a sub-stoichiometric value ($TiC_{0.57}$) corresponding to thermodynamic equilibrium with the C-saturated Ti matrix. The reaction rate is very fast and the solid-state reaction is almost complete after only a few minutes at 1073K (800°C) for the smallest particles, whereas the rate-limiting step remains the particle size. In addition, modeling of the diffusion processes in MMCs, i.e. initial dissolution of particles and their trend towards equilibrium composition, was performed using three particles size classes and the calculations were performed using the ThermoCalc and Dictra package. First, dissolution of the smallest particles (10% of the initial $TiC_{0.96}$

To cite this paper : *J. Andrieux, B. Gardiola, O. Dezellus, Synthesis of Ti matrix composites reinforced with TiC particles: in-situ synchrotron X ray diffraction and modeling, Journal of Materials Science 2018, Accepted for publication, doi 10.1007/s10853-018-2258-8.*

particles) is expected to be achieved after only 1s at 800°C. Second, the change in TiC composition lead to an increase in the total amount of carbide in the composite from 16 mass% to 19 mass%. The consequences on the industrial process of Ti/TiC MMC synthesis have also been considered. A typical industrial heat treatment of a MMC billet, 1h at 900°C, was modeled and the results showing an increase of the total amount of carbide in the composite from 16 mass% to 22 mass% are in rather good agreement with the experimental value (21 mass%). This highlights the potential of thermodynamic and kinetic modeling to help understand and optimize industrial processes for MMC synthesis.

**Keywords :** Metal matrix composites (MMCs); Solid state reaction; Interface Interdiffusion; Synchrotron diffraction; Theory and modeling (kinetics, transport, diffusion).

## 1. Introduction

The high specific mechanical properties of Metal Matrix Composite (MMC) lead to much considerations over the past decades for structural lightening in aerospace applications or wear resistance in car breaks. Among the different materials used as reinforcement for Titanium based MMC, titanium carbide (TiC) was selected for its excellent chemical compatibility with the matrix [1–4]. The powder metallurgy route, that is widely used to produced Ti-based MMC [5], leads to the preparation of green compacts where Ti and stoichiometric TiC are not in thermodynamic equilibrium before the consolidation of the MMC. During the heating step, an interfacial reaction between Ti and TiC will occur as already shown and studied in the literature [6, 7]. More precisely, a preceding paper gave details of the general scenario of chemical interaction between the Ti matrix and the TiC particles during the consolidation step at high temperature [8]. Four key steps were proposed starting with dissolution of the smallest particles to reach C saturation in the Ti matrix, followed by a change in the TiC stoichiometry in order to reach thermodynamic equilibrium between matrix and reinforcement following reaction (1):

$$y\,TiC + (1-y)\,Ti \rightarrow TiC_y \qquad (1)$$

According to the assessment of the C-Ti binary system by Dumitrescu et al., the phase equilibrium is characterized by a *y* value ranging from 0.55 to 0.595 at 1000°C and 600°C respectively [9]. Reaction 1 corresponds to incorporation of Ti from the metallic matrix to the

carbide phase. The reaction is therefore associated with two major phenomena: an increase in the total amount of reinforcement in the composite material and an increase in the mean particle radius by a factor of 1.19 [8]. As a consequence, the average distance between the particles decreases during the course of the reaction and contact between individual particles occurs in the most reinforced domain of MMC. This initiates an aggregation phenomenon that is responsible for the high growth rate of particles observed for heat treatment times lower than 1h. Finally, Ostwald ripening is responsible for the change in particles for longer heat treatment times [8].

The present work is focused on the two first steps, i.e. C saturation of the Ti matrix and the change in TiC stoichiometry resulting in the Ti-TiC composite material tending towards its thermodynamic equilibrium. The main objectives are an experimental determination of the kinetics of these two first steps, supported by a modeling of the diffusion phenomena occurring at the interface between a particle and the matrix. For this purpose, the reaction was investigated by in-situ synchrotron X-ray Diffraction (XRD) with a high-energy monochromatic X-ray beam at the European Synchrotron Radiation Facility (ESRF – ID15B). Nowadays, it is quite common in metallurgy to perform simulations of phase formation and transformations by using software packages such as DICTRA [10]. Such calculations require the use of two databases. The first is a thermodynamic database that can provide a good description of the system; from the point of view of both phase equilibria, and energetic description of the different phases of the system. The second is a mobility database that is needed to calculate the diffusion coefficient inside the main phases of the system. To the authors' knowledge, despite the great success of such calculations in describing metallurgical processes, the same approach has not been used for the synthesis of Metal Matrix Composites, despite the fact that the two types of materials can be considered as very similar. In the present study, the change in the Ti matrix and its TiC reinforcement over several heat treatment periods is simulated with the DICTRA package in order to compare the results with the experimental study by in-situ X-ray diffraction. As usual, if the simulations are able to reproduce experimental results obtained in well-controlled conditions, then they can also be used to extrapolate and predict microstructure changes in much more severe conditions.

To cite this paper : *J. Andrieux, B. Gardiola, O. Dezellus, Synthesis of Ti matrix composites reinforced with TiC particles: in-situ synchrotron X ray diffraction and modeling, Journal of Materials Science 2018, Accepted for publication, doi 10.1007/s10853-018-2258-8.*

## 2. Experimental procedures

### 2.1 Sample preparation

The starting materials used to prepare powder compacts were commercial $TiC_{0.96}$ and Ti powders (see Tables 1 to 3 for their compositions). Small cylinders of powder compacts (3 mm diameter and 2 mm height) characterized by a reinforcement content of 15vol.% TiC (16.23 mass%) were prepared by cold unidirectional pressing with a typical load of 1200 MPa in a tungsten carbide (WC) matrix.

| | Element concentration (mass%) | | | | | | |
|---|---|---|---|---|---|---|---|
| | Ti | Al | V | Fe | C | O | N |
| Ti grade2 powder | Balance | - | - | 0.0164 | <0.10 | 0.16 | <0.10 |

**Table 1** Chemical analysis of the Titanium powder used as starting material (SCA-CNRS Solaize)

| | Element concentration (in mass%) | | | | | | |
|---|---|---|---|---|---|---|---|
| | Total C | N | O | Fe | Cr | V | Mo |
| $TiC_{0.96}$ (starting powder) | 19.74 | 0.18 | 0.69 | 0.13 | 0.096 | 0.82 | <0.05 |

**Table 2** Chemical analysis of the $TiC_{0.96}$ powder used as starting material (SCA-CNRS, Solaize)

| | Element concentration (ppm in mass) | | | | | |
|---|---|---|---|---|---|---|
| | Fe | Cr | V | Ni | Ca | Cu, Cl, K, Zn, S, Er, As |
| $TiC_{0.96}$ (starting powder) | 1200 | 118 | 170 | 116 | 77 | traces |

**Table 3** X-ray fluorescence analysis of the $TiC_{0.96}$ powder used as starting material (SCA-CNRS, Solaize)

### 2.2 STEM characterization

Sample for STEM characterization was placed in a liquid tight graphite crucible and then immersed for 1 min in a liquid aluminium bath hold at 900°C. After 1min, the crucible was quenched in water. STEM characterization was performed on a JEOL-JEM 2100F microscope in Bright field mode, under an accelerating voltage of 200 kV and with a magnification of x40000.

### 2.3 In-situ experiments

#### 2.3.1 Heat treatment

The small cylinders of powder compacts were inserted under argon in a graphite crucible previously filled with a layer of Ti powder that was used as a getter for gaseous impurities such as oxygen or nitrogen. The graphite crucible was heated by an induction coil under vacuum (~$10^{-4}$ mbar) using an induction furnace available at ESRF through the Sample Environment Support Service (SESS). The temperature was measured and controlled using a K-type thermocouple placed in the crucible and connected to a 2408i Eurotherm controller. In step mode, the heating rate was measured at 60K.$s^{-1}$ with temperature stabilization of ±1K at 1273K (1000°C). The starting time of the experiment, t=0, corresponds to the beginning of the heating step.

#### 2.3.2 Synchrotron XRD

Transmission X-Ray Diffraction (XRD) experiments were performed on beamline ID15B at ESRF (Grenoble) using a high-energy X-ray monochromatic beam (300x300 $\mu m^2$) with a wavelength of 0.14370 Å (~86.3 keV) and a $\Delta E/E \sim 10^{-4}$. To follow small variations in the diffraction peak position and improve the angular resolution ($\Delta(2\theta)$=0.003 °($2\theta$)), the sample-detector distance was increased to 4.358 meters, leading to a cell parameter resolution of $\Delta a$=0.002 Å. In addition, the detector was off-centered by 200 mm compared to the direct beam to select a $2\theta$ range from 2.8 to 5°($2\theta$) and to focus the acquisition on the main TiC diffraction peaks, i.e. the (111)-3.295°$2\theta$ and the (200)-3.806°$2\theta$ peaks. Continuous acquisitions were performed using a MAR345 detector with an exposure time of 90s. Thus, diffraction rings were radially integrated using Fit2D software [11]. An example of a diffraction pattern collected on the sample at room temperature with peak identification is given in Figure 1.

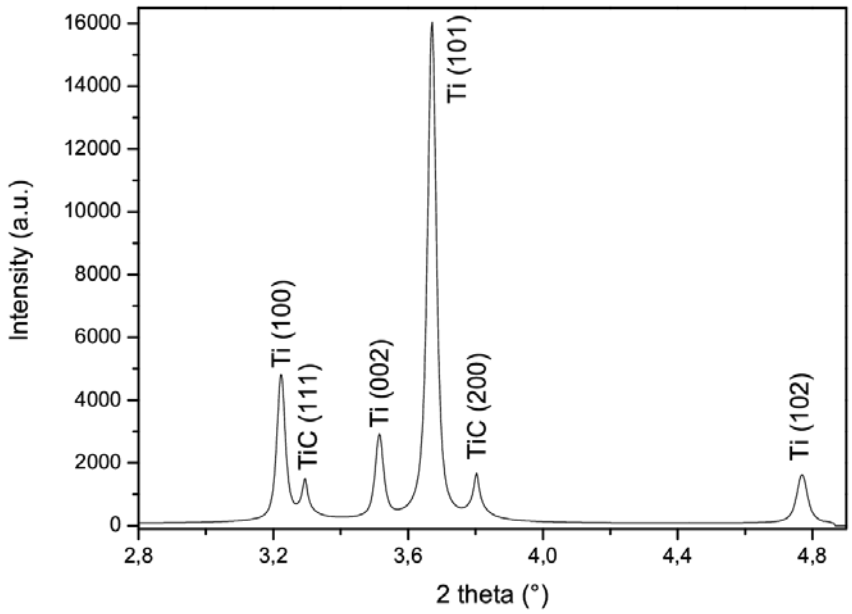


**Fig. 1** Example of diffraction pattern collected from the sample at room temperature with peak identification

2.4 Sequential Rietveld refinement

The structural study was performed by sequential Rietveld refinement using the FullProf Suite Software with the WinPlotr graphical interface [12, 13]. The profile function 7 in Full Prof, a Pseudo-Voigt function with axial divergence correction, was used. The instrument resolution file was defined using $LaB_6$ as standard. Following the reduced $2\theta$ range of acquisition due to the experimental configuration and the aim of the present paper, the Rietveld refinement was only performed on TiC diffraction peaks. For each refinement process, the refinement weighting factors were found at maximum $R_p$<15%, $R_{wp}$<20%, $R_{exp}$<10%, $\chi^2$<5. More details in the sequential Rietveld refinement procedure are given in Section 3.1.

## 3. Experimental Results

3.1 Rietveld refinement

Titanium carbide has a halite structure (two face-centered cubic (fcc) sublattices with Ti and C, respectively). It displays deviations in stoichiometry over a wide range of homogeneity, from $TiC_{0.47}$ to $TiC_{0.99}$, because of the presence of vacancies in the carbon sublattice [14]. Consequently, this phase is usually modeled in Calphad assessments by using the compound

energy formalism with two sublattices having the same number of sites, one totally filled by Ti atoms, the other filled by a random mixture of C atoms and vacancies [9, 15, 16] leading to a chemical formula that can be expressed as $TiC_y$ in order to illustrate both the stoichiometry range and the location of vacancies on the C sublattice. Experimentally, the number of vacancies has a conspicuous effect on the lattice parameter. In a review of the Group 4a carbides, Storms [17] reported that the lattice parameter expands for $0.99 > y > 0.85$ and shrinks for $0.85 > y > 0.5$, the total change in lattice parameter being less than 1%, from 4.330nm to 4.298nm respectively [18–26]. The unusual presence of a maximum in the lattice parameter vs. composition curve, corresponding to anomalous volume behavior of TiC at small vacancy concentration, was recently explained by Hugosson as resulting from an effect of local relaxation of the atoms surrounding the vacancy sites [27]. Consequently, changes in *y* of the $TiC_y$ phase are associated with a slight modification in both the lattice parameter (about 1%) and the peak intensities because of variations in the number of vacancies in the C sublattice. Thanks to the improved angular resolution of the present in-situ XRD study ($\Delta a$=0.002 Å), these variations were captured and analyzed by Rietveld refinement to follow in situ the pathway to equilibrium during heat treatment of a Ti-TiC composite material.

The $TiC_{0.96}$ particles used as starting material present a continuous particle size distribution ranging over three decades from 15-20 nm for the smallest to 7-10 µm for the biggest [8], leading to different crystallite sizes, with constant starting stoichiometry (Table 2) and lattice parameters. Diffraction peaks of such a population of particles are characterized by a convolution of different contributions due to the different crystallite sizes at the same $2\theta$ position: a sharp and intense peak due to the biggest particles (i.e. a mean diameter value of about 1 µm) and a broader peak due to the smallest particles (a few tenths of nm), leading to a broadening at the bottom of the TiC diffraction peak, as evidenced on Figure 2.a. This specific peak shape was fitted during Rietveld refinement by using two populations of TiC particles: the first, labeled "$TiC_{0.96}$_SC", presents a small crystallite size and is related to the smallest particles whereas the second, labeled "$TiC_{0.96}$_BC", is associated with the biggest particles. An example of a Rietveld refinement result of (200) TiC peak is given in Figure 2.a. During the sequential

Rietveld refinement, the chemical composition of these two populations corresponding to the starting material (i.e. C and Ti site occupancies) was fixed and kept constant whereas the intensity scale factor, the peak shape profile parameters and the lattice parameters were refined independently. In terms of temperature, the diffraction peaks associated with $TiC_{0.96}$_BC and $TiC_{0.96}$_SC shifted to lower $2\theta$ values due to thermal expansion. In addition, new diffraction peaks were observed for a higher value of $2\theta$ and associated with the formation of the sub-stoichiometric $TiC_y$ phase, labeled "$TiC_y$". During the sequential Rietveld refinement, the composition, the intensity scale factor, the peak shape profile parameters and the lattice parameters of the $TiC_y$ phase were refined. An example of Rietveld refinement of (200) TiC diffraction peaks acquired at 900°C is given in Figure 2.b.

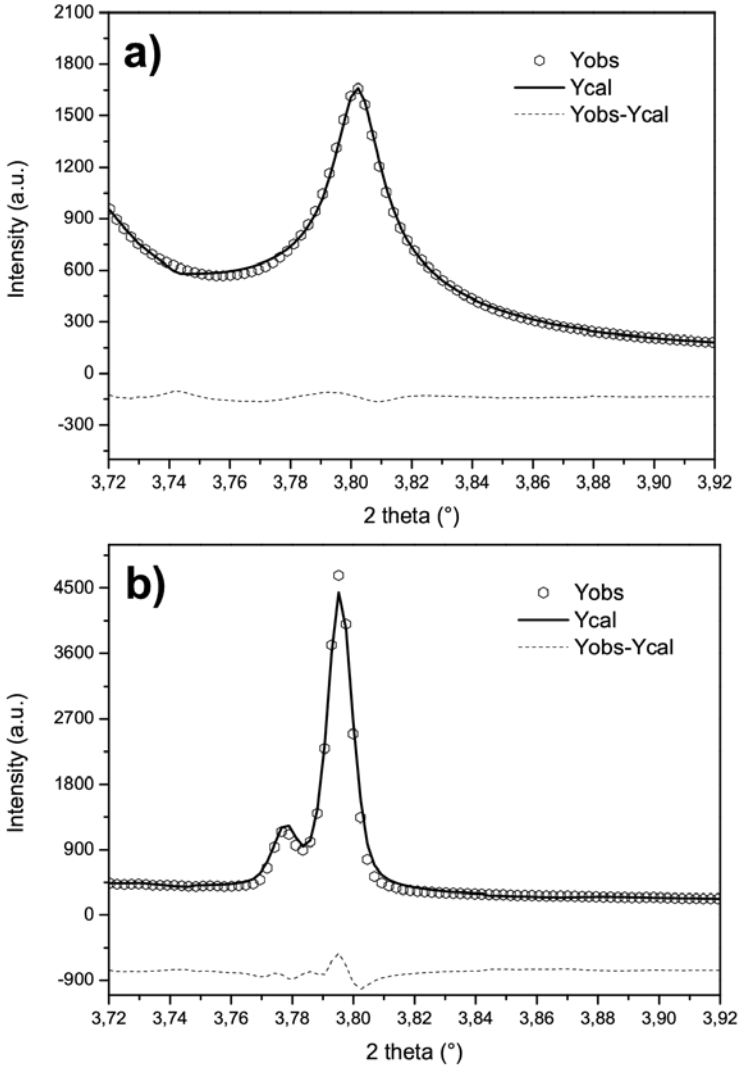


**Fig. 2** Rietveld refinement of (200) TiC peak, a) room temperature XRD acquisition ($R_p$=12.9%; $R_{wp}$=12.8%; $R_e$=9.15%; $\chi^2$=1.96); b) XRD acquisition performed at 900°C ($R_p$=8.5%; $R_{wp}$=8.3%; $R_e$=6.1%; $\chi^2$=1.85).

To cite this paper : *J. Andrieux, B. Gardiola, O. Dezellus, Synthesis of Ti matrix composites reinforced with TiC particles: in-situ synchrotron X ray diffraction and modeling, Journal of Materials Science 2018, Accepted for publication, doi 10.1007/s10853-018-2258-8.*

### 3.2 Isothermal heating at 1073K (800°C) for 2h

#### 3.2.1. Raw data

The time-dependent change in the TiC(200) peak during isothermal heating at 1073K (800°C) is shown on Figure 3. The colorscale is related to the peak intensity. Note that the darker area around 4500s was due to synchrotron beam refill. It can be clearly seen from Figure 3 that a new diffraction peak appears at higher $2\theta$ values for the TiC(200) peak, corresponding to the formation of a TiC population with smaller cell parameters, i.e. a sub-stoichiometric composition $TiC_y$. The peak position of the $TiC_y$ composition remains constant as a function of time at 1073K (800°C), meaning that the lattice parameter and therefore the stoichiometry of the phase, remain constant. Finally, the intensity of the $TiC_y$ diffraction peak increases whereas that of the starting $TiC_{0.96}$ population decreases. Note that the same results were observed with the TiC(111) peak.

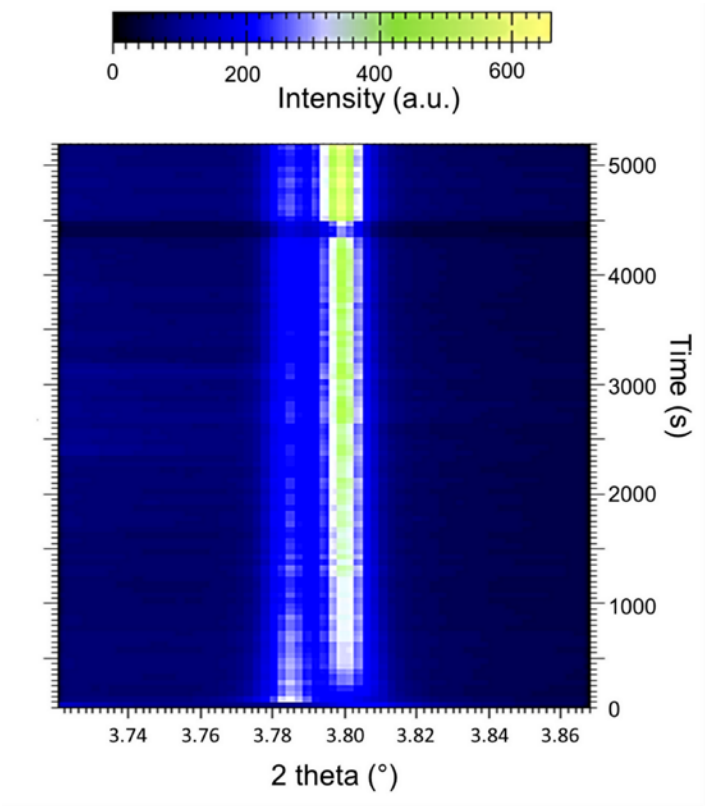


**Fig. 3** Time-dependent change in the TiC(200) during isothermal treatment at 1073K (800°C). The colorscale indicates the peak intensity (on-line version).

3.3.2. Rietveld refinement results

The time-dependent change in cell parameter is given on Figure 4. Note that t=0 on Figure 4 corresponds to the beginning of the heating step. First of all, this figure confirms the presence during the whole process of only two populations of TiC, characterized by two distinct values of lattice parameters. From a lattice parameter $a_{RT}$=4.330Å at room temperature, the initial population corresponding to $TiC_{0.96}$ has a parameter of $a_{800°C}$=4.353 Å at 800°C and this cell parameter remains stable during the course of reaction 1. It may be deduced that the cell expansion for the $TiC_{0.96}$ due to the temperature increase is $\Delta a$=0.023 Å. Concerning the $TiC_y$ population that forms at high temperature, Figure 4 shows an almost constant lattice parameter of $a_{TiCy@800°C}$=4.336Å, the variation being less than 0.02% during the experiment.

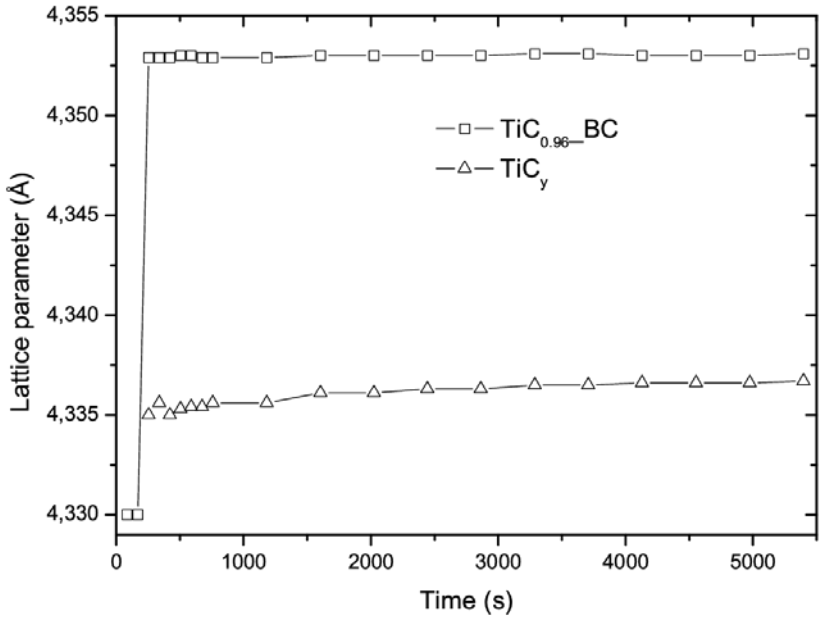


**Fig. 4** Time-dependent change in cell parameter during isothermal treatment at 800°C. t=0 corresponds to the beginning of the heating step.

Assuming that the thermal expansion is the same for $TiC_{0.96}$ and $TiC_y$, the lattice parameter of the $TiC_y$ population at RT can be estimated to be equal to $a_{TiCy@RT}$=4.314Å. Following the correlation between the cell parameter and the stoichiometry of $TiC_y$ reported by Storms [17], the composition of the $TiC_y$ population is found to be $TiC_{0.57}$. This experimental determination of the $TiC_y$ composition that forms at high temperature is in good agreement with the value

expected when thermodynamic equilibrium is reached between the carbide and Ti phase at 1073K (800°C) [8, 9].

The formation of a sub-stoichiometric $TiC_y$ phase is confirmed at the interface between $TiC_{0.96}$ particles and the Titanium matrix as illustrated on STEM micrograph of a selected zone of the MMC microstructure (Figure 5). It leads to a core-shell structure of the particles, with a stoichiometric TiC core and a $TiC_y$ shell, in accordance with bright field mode contrasts.

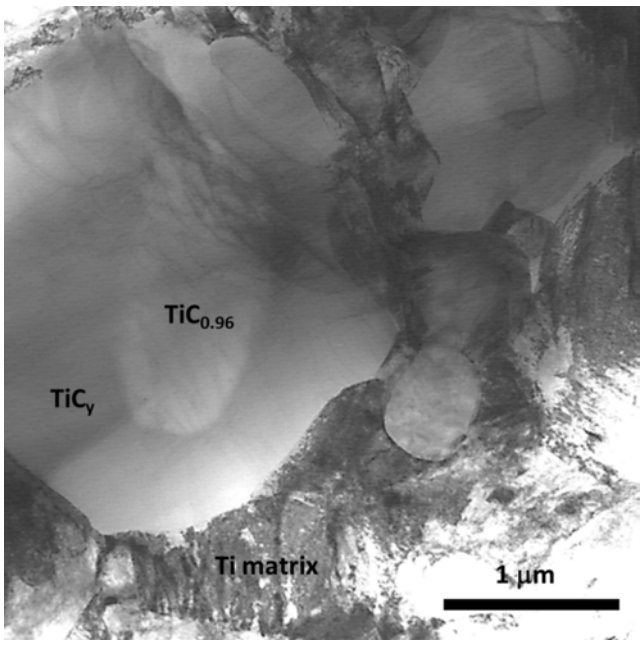


**Fig. 5** Bright field STEM view of core-shell microstructure of TiC particles in Ti-TiC MMC, obtained after 1min at 900°C.

Figure 6 presents the time-dependent variation in the amount of the three identified populations of TiC particles (see Section 3.1) during isothermal annealing at 1073K (800°C). As already observed in Figure 3, the quantity of the $TiC_y$ population increases whereas that of the initial $TiC_{0.96}$ composition decreases. More interestingly, the population of the initial smallest crystallites ($TiC_{0.96}$_SC) is consumed after only 3 min of heat treatment. In addition, 50% conversion of $TiC_{0.96}$_BC into $TiC_y$ phase is reached after only 6min of heat treatment. Finally, after 1h30 at 1073K (800°C), a complete reaction is not observed as ~25 % of $TiC_{0.96}$_BC remains in the sample.

To cite this paper : *J. Andrieux, B. Gardiola, O. Dezellus, Synthesis of Ti matrix composites reinforced with TiC particles: in-situ synchrotron X ray diffraction and modeling, Journal of Materials Science 2018, Accepted for publication, doi 10.1007/s10853-018-2258-8.*

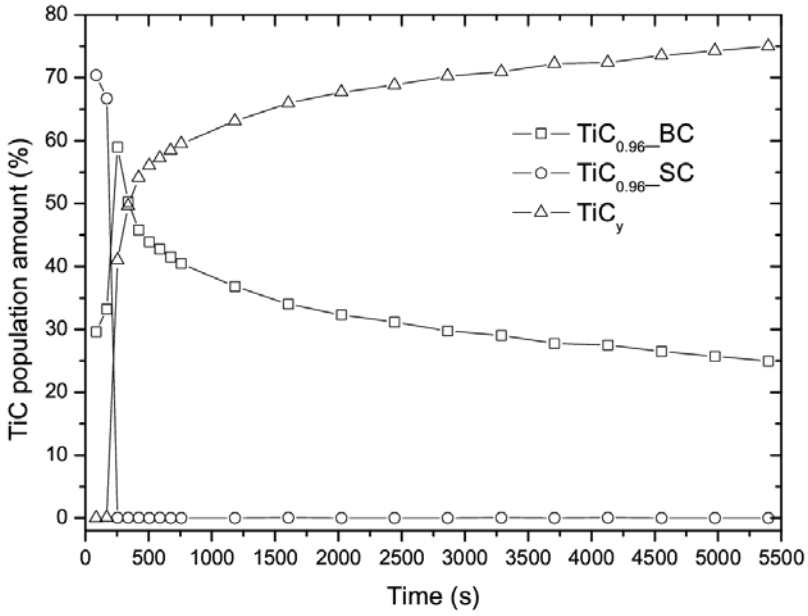


**Fig. 6** Changes in the quantity of different populations of TiC calculated using Rietveld refinement during isothermal treatment at 800°C. t=0 corresponds to the beginning of the heating step.

In order to improve the angular resolution, and thus be able to detect two populations of TiC with different lattice parameters, the sample-detector distance was increased. As a consequence, because of the restricted number of diffraction peaks detected, a quantitative analysis to monitor the mass fraction of reinforced TiC in the MMC was not directly possible by Rietveld refinement. However, considering that the amount of C initially present in the $TiC_{0.96}$ phase is constant during the experiment and distributed between the two TiC populations, stoichiometric and substoichiometric ($TiC_{0.96}$ and $TiC_{0.57}$ respectively) and in the saturated Ti matrix, the whole mass fraction of TiC phase, $M_{TiC}$, can be estimated from the XRD results by applying equation (1).

Eq. 1
$$M_{TiC} = \frac{M^{ini}_{TiC_{0.96}} . y^{C}_{TiC_{0.96}} - M^{ini}_{Ti} . y^{C}_{Ti}}{Q_{TiC_{0.96}} . y^{C}_{TiC_{0.96}} + Q_{TiC_{0.57}} . y^{C}_{TiC_{0.57}}}$$

with $M^{ini}_{TiC0.96}$= initial mass fraction of $TiC_{0.96}$ in the MMC; $M^{ini}_{Ti}$= initial mass fraction of Ti in the MMC; $Q_{TiC0.96}$ = amount of $TiC_{0.96}$; $Q_{TiC0.57}$ = amount of $TiC_{0.57}$; $Y^{C}_{TiC0.96}$= weight fraction of C in $TiC_{0.96}$; $Y^{C}_{TiC0.57}$= weight fraction of C in $TiC_{0.57}$; $Y^{C}_{Ti}$= weight fraction of C in the saturated Ti matrix;

The total mass fraction of reinforced TiC in the composite, calculated using equation (1), based on the experimental results obtained during the isothermal experiment at 1073K (800°C), is presented in Figure 7 (filled circles). The calculated mass fraction of reinforced TiC in the composite is of major concern as it is a key parameter governing the expected mechanical properties of the MMC.

As the in-situ experiment time was set to 3600s, final equilibrium was not reached but extrapolation based on total conversion of the initial stoichiometric population to the substoichiometric composition determined by XRD provides a means of estimating the equilibrium mass fraction of TiC that is found to be equal to 0.2303 (dashed-dotted horizontal line on Figure 7). This value is in good agreement with that expected after thermodynamic equilibrium is reached (0.2306).

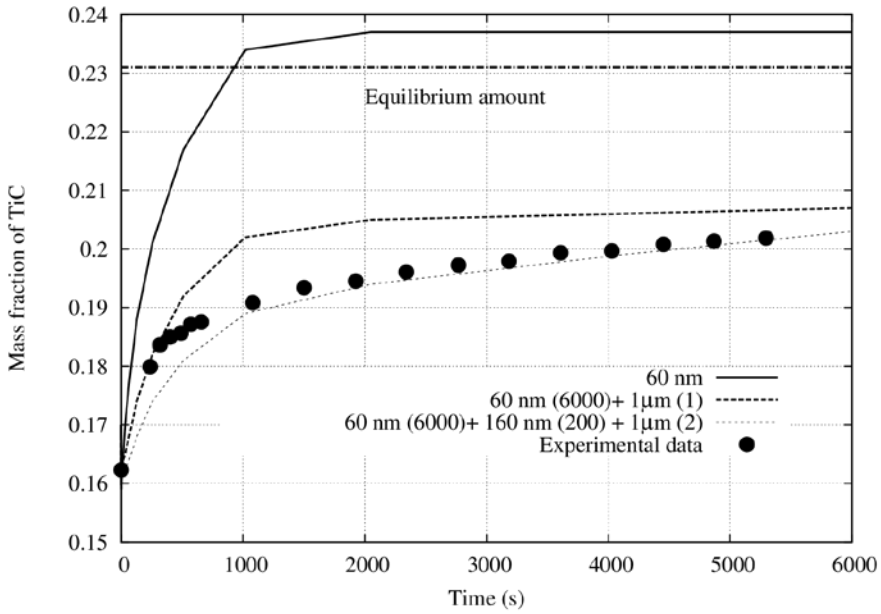


**Fig. 7** Calculated time-dependent change in the mass fraction of TiC particles in a Ti matrix during isothermal heat treatment at 1073K (800°C). The solid line corresponds to one class of particles with a unique TiC diameter of 60nm. The dashed line shows the results obtained with two classes of TiC particles with different diameters: 6000 particles of 60nm, and one particle of 1µm. The dotted line corresponds to three classes of particles: 6000 particles of 60nm, 200 particles of 160nm and two particles of 1µm. The experimental values and the final asymptotic amount of TiC are also reported (filled circles and dashed-dotted horizontal line respectively).

To cite this paper : *J. Andrieux, B. Gardiola, O. Dezellus, Synthesis of Ti matrix composites reinforced with TiC particles: in-situ synchrotron X ray diffraction and modeling, Journal of Materials Science 2018, Accepted for publication, doi 10.1007/s10853-018-2258-8.*

## 4. Modeling

### 4.1 Simulation conditions

In order to model the changes that take place in the Ti-TiC metal matrix composite during high temperature heat treatment, the DICTRA software package [28] was used. DICTRA stands for diffusion-controlled transformation and is based on a numerical solution of the multicomponent diffusion equations and local thermodynamic equilibrium at the phase interfaces. The program is suitable for treating phenomena such as growth [29], dissolution [30] and coarsening of particles in a matrix phase [31]. The DICTRA software package is built with databases for thermodynamics and diffusion. The present simulations were performed using the MOB2 mobility database provided by the ThermoCalc company and the thermodynamic assessment of the C-Ti system published by Dumitrescu et al. [9].

The simulations were performed considering a spherical geometry, representative of reinforcing particles embedded in a metallic matrix. The carbide particle was defined as being spherical with an initial radius $R_{TiC}$ at the center of a spherical cell of radius $R_{Mat}$ defined by the surrounding metallic matrix (see Figure 8).

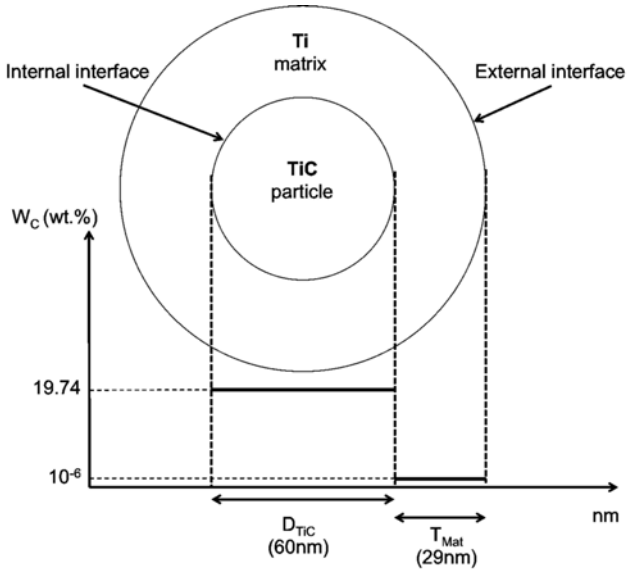


**Fig. 8** Schematic model of the initial configuration of the system used in the DICTRA simulations

The first key step of the DICTRA simulations is to give values to the parameters of the geometrical configuration shown in Figure 8, i.e. the TiC particle diameter and the subsequent Ti shell thickness. According to Figure 9, the main diameter of $TiC_{0.96}$ particles removed from

To cite this paper : *J. Andrieux, B. Gardiola, O. Dezellus, Synthesis of Ti matrix composites reinforced with TiC particles: in-situ synchrotron X ray diffraction and modeling, Journal of Materials Science 2018, Accepted for publication, doi 10.1007/s10853-018-2258-8.*

the composite powder after the ball-milling step, before any high temperature treatment, is estimated to be $D_{TiC}$ = 128 nm. However, the residual presence of a tail corresponding to micron-sized particles must be taken into account. Note that the volume of matter corresponding to a 1µm particle is equivalent to 1000 particles or 8000 particles of respectively 100 and 50nm in size. It is difficult to obtain the real size distribution by counting particles from SEM observations because the quantity of biggest particles will be systematically overestimated. Therefore, the size distribution will be used as a guide giving the main trends, but exact numerical values cannot be used for modeling.

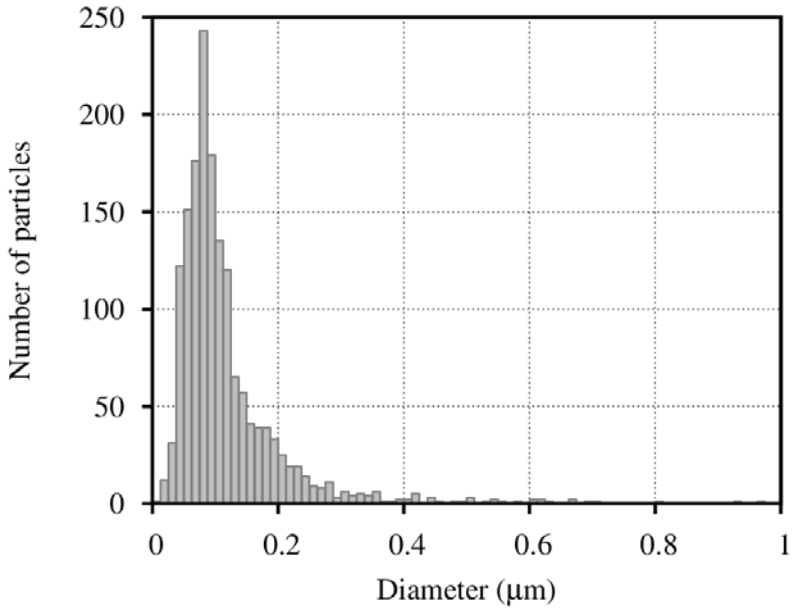


**Fig. 9** Diameter distribution of $TiC_{0.96}$ particles removed from the composite powder by selective acid etching after a ball-milling step and before any high temperature treatment.

As a consequence, the initial size of $TiC_{0.96}$ particles in the model was estimated from Figure 6 and more precisely from the volume ratio, *r*, between untransformed and transformed populations of TiC, respectively $TiC_{0.96}$ and $TiC_{0.57}$ populations. During the heat treatment, each particle can be considered as a core-shell structure with the residual $TiC_{0.96}$ composition as a core of radius *R* and the modified $TiC_{0.57}$ stoichiometry as a shell of thickness *e*. Given that the transformation occurs by a solid state diffusion process through the external shell, its thickness *e* depends only on the time of interaction and can be estimated by equation (2) regardless of the initial particle size ($D_{inter}$ is the interdiffusion coefficient in $TiC_{0.57}$).

Eq. 2 $$e = \sqrt{D_{inter} t}$$

The ratio *r* of the core to shell volumes for a spherical particle, corresponding to the advancement of the reaction transforming the particle, is then given by equation 3:

Eq. 3 $$r = \frac{R^3}{(R+e)^3 - R^3}$$

The radius of the residual inner $TiC_{0.96}$ core can then be estimated for a given diffusion time *t* and advancement of reaction *r* following equation (4):

Eq. 4 $$R = \frac{\sqrt{D_{inter} t}}{\left(\frac{1+r}{r}\right)^{\frac{1}{3}} - 1}$$

This equation can be used to estimate, for a given interaction time *t*, the radius of the residual $TiC_{0.96}$ core, leading to a given advancement of reaction *r*. According to Figure 6, the residual amount of the initial $TiC_{0.96}$ population is about 50% (*r* = 0.5) after t = 400s at 1073K (800°C). The interdiffusion coefficient reported by van Loo et al. at this temperature for $TiC_{0.57}$ is equal to $2.58 \times 10^{-19}$ $m^2.s^{-1}$ [32]. Therefore, numerical applications lead to a shell thickness *e* = 10nm and a core radius *R* = 23 nm.

From these simple calculations, it may be concluded that, considering a single particle size distribution, the very fast transformation rate of the initial $TiC_{0.96}$ composition can only be obtained for particles with an initial radius smaller than the typical value of about 30 nm. As a consequence, an initial TiC particle radius of 30nm is used for modeling (diameter equal to 60nm).

In the model, the thickness of the metallic shell in which the carbide particle is embedded is fixed in order to obtain a massive amount of reinforcement equal to 16.23 mass%, i.e. a value corresponding to the composite material experimentally studied. In the case of carbide particles with a diameter of 60 nm, this consideration leads to a Ti matrix shell thickness of 29 nm. To model the isothermal treatment at 1073K (800°C), the matrix and particle domains are considered as being respectively the HCP_A3 phase with an initial C mass fraction of $10^{-6}$ (see table 2), and the carbide $TiC_{0.96}$ phase with a starting C composition of 19.74 mass%C (Table 3).

4.2 Simulation results: isothermal treatment at 1073K (800°C)

The first step observed by in-situ XRD during the isothermal treatment at 1073K (800°C) is the dissolution of the smallest particles. This is revealed by the disappearance of the broadening of the bottom part of the diffraction peaks mentioned on Figure 2. This phenomenon can be related to C saturation of the Ti matrix that is achieved by partial dissolution of the initial amount of $TiC_{0.96}$ carbide and particularly the smallest particles. From the modeling, this dissolution step can be illustrated both by the time needed to reach saturation at the external interface of the Ti matrix (Figure 10.a) and by the time corresponding to attainment of a minimum TiC mass fraction, after dissolution and before growth (Figure 10.b).

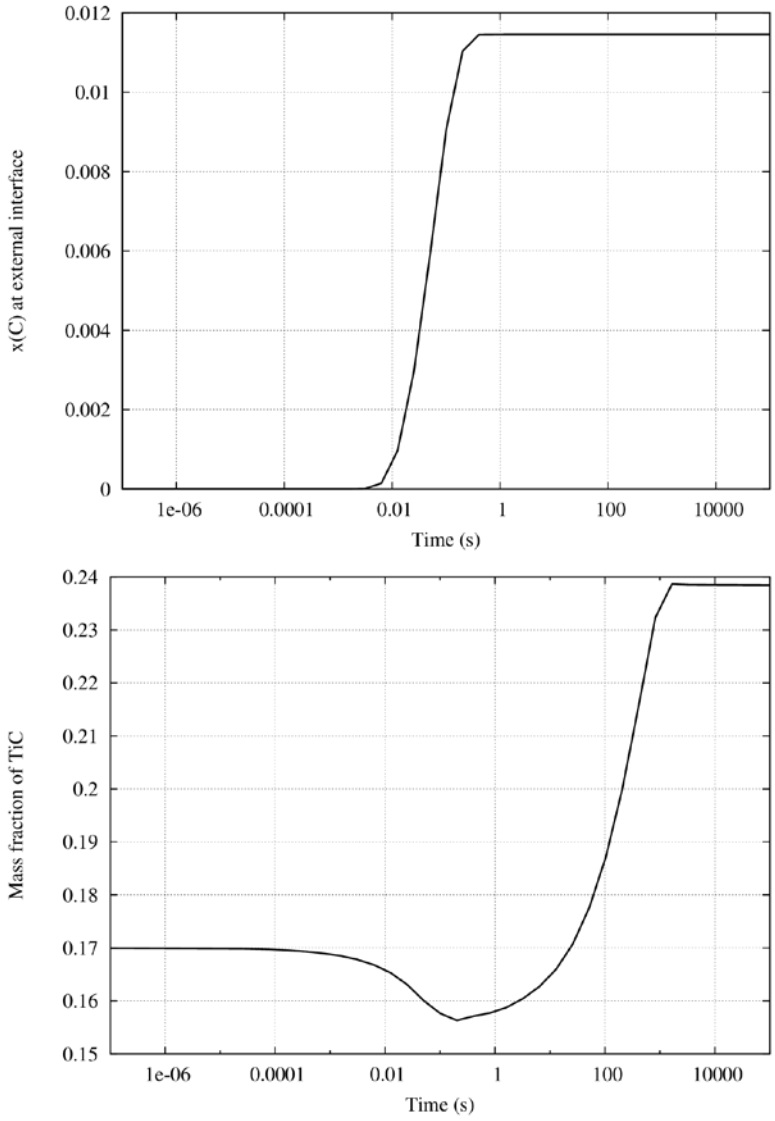


**Fig. 10** (a) Time-dependent change in the C content at the external Ti matrix interface during isothermal treatment at 1073K (800°C). (b) Time-dependent change in the calculated mass fraction of TiC particles in the Ti matrix at the very beginning of the isothermal treatment, during the dissolution step.

Figures 10.a and b indicate that the dissolution of the smallest particles in order to allow carbon saturation of the Ti matrix is expected to be achieved after a typical isothermal time at 1073K (800°C) of about 1 s. This result should be compared with Figure 6 where the Rietveld refinement of diffraction peaks shows the disappearance of the population of smallest particles after about 100 s. Obviously, some discrepancies are to be expected for such short times as the experimental heating rate is finite (i.e. $60K.s^{-1}$), even if a step function toward 1073K (800°C) was used for the induction heater and for calculations. Therefore, the typical times of the experimental results are expected to be slightly higher than those obtained from the kinetics calculations. More precisely, a careful analysis of Figure 4 reveals that the thermal expansion of the initial population of stoichiometric $TiC_{0.96}$ particles is observed experimentally in the center of the sample a few hundreds of seconds after starting the induction heater. Considering these limitations in the comparison of the shortest characteristic times for experiments and calculations, the agreement is relatively good and illustrates that chemical exchanges and solid state diffusion of C in the Ti matrix are extremely fast.

The solid line in Figure 7 presents the calculated change in the TiC mass fraction as a function of treatment time at 800°C in the case of $TiC_{0.96}$ particles with a unique size of 60 nm diameter. The experimental mass fraction of TiC determined from the in-situ experiments is also reported (filled circles). The model correctly reproduces the fast increase in the TiC mass fraction observed by XRD in-situ measurements at the beginning of heat treatment. However, with a unique size of 60 nm, the final equilibrium is almost reached after only 1000 s whereas, experimentally, equilibrium is still not obtained after 3600s. As previously noted, the presence after milling of residual micron-sized particles is responsible for the experimentally observed two-step change: fast conversion of the smallest particles and much slower conversion of the biggest particles.

Given that diffusion processes control the change in the amount of TiC particles, this change is therefore limited by the presence of the few big particles with the initial $TiC_{0.96}$ composition remaining in the TiC population after milling. Therefore, in order to improve the modeling process and to illustrate the drastic influence of the residual presence of big particles, the same calculation was performed with a 1µm size particle and associated with the preceding results by

a simple linear combination. The relative amount of the two classes of particles is defined in order to get a 50% volume fraction of the smallest class, a value that should allow the initial fast reaction rate to be captured. Calculation results are reported in Figure 7 with a dashed line. As expected, the presence of one micron-sized particle, in association with 6000 particles with a diameter of 60nm, allows the capture of both the initial transformation rate and the asymptotic trend towards the equilibrium state. Note that just one micron-sized particle represents 38% of the total volume of particles in the sample.

Finally, to illustrate the potential of thermokinetic modeling, a third class is added with an intermediate size of 160nm in diameter and the results are presented in Figure 7 with a dotted line (population in numbers are 6000, 200 and 2 for 60, 160 and 1000nm sized respectively).

## 5. Discussion

The present results highlight the fast kinetics of the trend towards thermodynamic equilibrium of a Ti-based matrix composite reinforced by $TiC_{0.96}$ particles. During isothermal treatment at 1073K (800°C), the dissolution of the smallest $TiC_{0.96}$ particles to reach saturation of the Ti matrix is obtained after a few tenths of a second, while the formation of the equilibrium composition of the carbide phase, $TiC_{0.57}$, concomitantly increases sharply. Moreover, after only 6min of isothermal treatment at 1073K (800°C), 50% of the conversion of TiC particles from their initial $TiC_{0.96}$ composition towards the equilibrium value, $TiC_{0.57}$, is achieved.

It is to be expected that such high reaction rates will have major consequences on the MMC synthesis process. First of all, reaching the C saturation of the Ti matrix induces the dissolution of about 10% of the initial $TiC_{0.96}$ particles (Figure 10.b). This dissolution process affects the smallest particles, which means that most of the effort made during milling to decrease the size of the initial particles is cancelled out. Next, the change in initial TiC composition ($TiC_{0.96}$) towards the equilibrium value ($TiC_{0.57}$) is achieved by partial conversion of the Ti matrix into carbide phase. This process therefore leads to an increase in the total amount of carbide in the composite from 16mass% to about 19mass% after 6min at 1073K (800°C) (Figure 7) and to an increase in particle size [8]. These changes induce a trend towards the formation of particle clusters that might have detrimental effects on the mechanical properties because of local embrittlement.

These two main processes, i.e. dissolution of the smallest particles and increase in total number of particles, occur during the industrial high temperature consolidation step of a Ti-based matrix composite reinforced by TiC particles. It is difficult to avoid them for two reasons: the driving force is thermodynamic and their kinetics is very fast. As a consequence, they have to be considered upstream in the process design: for example by reducing the initial quantity of TiC particles.

The reliability of thermokinetic modeling to simulate the change in TiC reinforcement in Ti-based composites has been demonstrated for the case of isothermal treatment (Figure 7). It can thus now be used to predict the change in mass fraction of reinforcement during the heat treatment that is performed prior to the consolidation step. Figure 11 presents a typical industrial heat treatment that involves inserting a billet, containing the cold compacted composite powder, inside a furnace heated to 1173 (900°C) for 1h. According to temperature measurements inside the consolidation furnace used for the experiment, the duration of the heating step is considered to be 10 min while the isothermal holding time is 50 min. The calculated change in TiC mass fraction, considering three particle size classes (as in Figure 7), is reported in Figure 11, as well as the experimental value determined just after the consolidation step. Once again, this figure highlights the fast kinetics of the reaction occurring inside the MMC as most of the transformation of the TiC stoichiometry, associated with the increase in particle mass fraction, is already achieved after a holding time of 10 min.

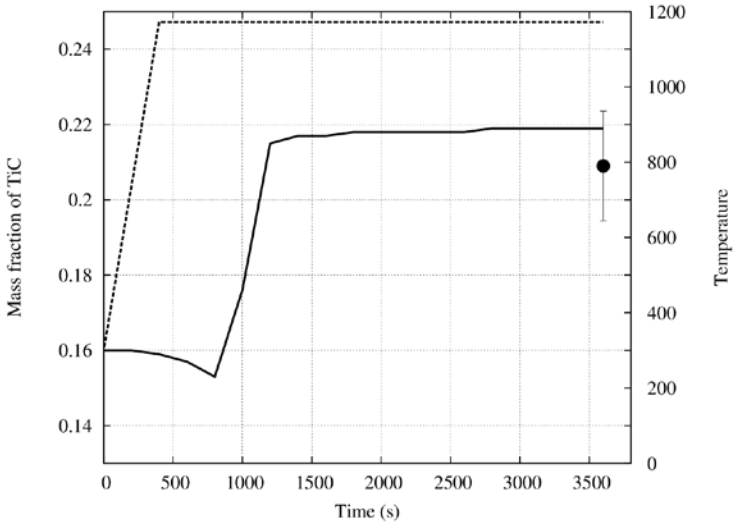


**Fig. 11** Change in the calculated TiC mass fraction during heat treatment of a composite powder compact prior to the consolidation step (solid line). Temperature vs time is also reported (dashed line) as well as the experimental mass fraction determined after heat treatment and the consolidation step (filled circle).

To cite this paper : *J. Andrieux, B. Gardiola, O. Dezellus, Synthesis of Ti matrix composites reinforced with TiC particles: in-situ synchrotron X ray diffraction and modeling, Journal of Materials Science 2018, Accepted for publication, doi 10.1007/s10853-018-2258-8.*

## 6. Conclusion

The reaction tending towards thermodynamic equilibrium during the synthesis of Ti/TiC MMC prepared by the powder metallurgy route was studied by in-situ synchrotron X-ray diffraction. It was found that the carbide composition changes rapidly from its initial stoichiometric composition $TiC_{0.96}$ towards a sub-stoichiometric value ($TiC_{0.57}$) corresponding to the thermodynamic equilibrium with the C saturated Ti matrix. The reaction is almost complete after only a few minutes at 800°C for the smallest particles, whereas the rate-limiting step is the particle size. Modeling of the diffusion processes in MMCs isothermal heat treatment at 800°C was performed using three particles size classes. First dissolution of the smallest particles (about 10% of the initial $TiC_{0.96}$ particles) is expected to be achieved after only 1s at 800°C. Second the change in TiC composition lead to an increase in the total amount of carbide in the composite from 16 mass% to 19 mass%. The consequences on the industrial process of Ti/TiC MMC synthesis have also been considered. Typical industrial heat treatment of a MMC billet, 1h at 900°C, was modeled and the results showing an increase of the total amount of carbide in the composite from 16 mass% to 22 mass% are in rather good agreement with the experimental value (21 mass%). This illustrates the potential benefits of thermodynamic and kinetic modeling, combined to in-situ X-ray diffraction, in understanding and optimizing industrial processes for MMC synthesis.

## Acknowledgements

This work was undertaken in the framework of the COMETTi project funded by the French national research agency (ANR) [grant number ANR-09-MAPR-0021]. O.D. is very grateful to Dr. S. Fries and Pr. I. Steinbach from ICAMS institute at Bochum University (Germany) for allowing DICTRA calculations on their informatics cluster. J.A. thanks ID15B beamline staff for their help during beam time and ESRF for the provision of beamtime through in-house research during his post-doctoral position. The authors thank Gilles RENOU for the STEM observation performed at the "Consortium des Moyens Technologiques Communs" (CMTC, http://cmtc.grenoble-inp.fr). Composite powders were provided by the Mecachrome company (www.mecachrome.fr).

**Conflicts of interest statement**

The authors declare that they have no conflict of interest.

**References**

1. Clyne TW, Withers PJ (1993) An introduction to Metal Matrix Composites, Cambridge University Press, Cambridge.

2. Lindroos VK and Talvitie MJ (1995) Recent advances in metal matrix composites, J Mater Process Tech 53:273-284.

3. Miracle DB (2005) Metal matrix composites – From science to technological significance, Compos Sci Technol 65:2526-2540.

4. Huang LJ, Geng L, Xu HY, Peng HX (2011) In situ TiC particles reinforced Ti6Al4V matrix composite with a network reinforcement architecture, Mat Sci Eng A-Struct 528:2859-2862.

5. Liu Y, Chen LF, Tang HP, et al (2006) Design of powder metallurgy titanium alloys and composites, Mat Sci Eng A-Struct 418:25-35.

6. Quinn CJ, Kohlstedt Dl (1984) Solid-State Reaction Between Titanium Carbide and Titanium Metal, J Am Ceram Soc 67:305-310.

7. Wanjara P, Drew RAL, Root J, Yue S (2000) Evidence for stable stoichiometric Ti2C at the interface in TiC particulate reinforced Ti alloy composites, Acta Mater 48:1443-1450.

8. Roger J, Gardiola B, Andrieux J et al (2017) Synthesis of Ti matrix composites reinforced with TiC particles: thermodynamic equilibrium and change in microstructure. J Mater Sci 52:4129-4141.

9. Dumitrescu LFS, Hillert M, Sundman B (1999) A reassessment of Ti-C-N based on a critical review of available assessments of Ti-N and Ti-C. Z Metallkd 90:534-541.

10. Andersson JO, Helander T, Höglund L et al (2002) Thermo-Calc & DICTRA, computational tools for materials science, Calphad 26:273-312.

11. Hammersley AP, Svensson SO, Hanfland M et al (1996) Two-dimensional detector software: From real detector to idealised image or two-theta scan, High Pressure Res 14:235-248.

12. Roisnel T, Rodríguez-Carvajal J (2001) WinPLOTR: A windows tool for powder diffraction pattern analysis, In: Materials Science Forum. Transtec Publications, pp 118-123.

13. Rodríguez-Carvajal J (1993) Recent advances in magnetic structure determination by neutron powder diffraction, Physica B 192:55-69.

14. Seifert HJ, Lukas HL, Petzow G (1996) Thermodynamic optimization of the Ti-C system. J Phase Equilib 17:24-35.

15. Jonsson S (1996) Assessment of the Ti-C system, Z Metallkd 87:703-712.

16. Frisk K (2003) A revised thermodynamic description of the Ti-C system, Calphad 27:367-373.

17. Storms EK (1962) A critical review of refractories. Part I. Selected properties of Group 4a, 5a and 6a carbides, Rept. no. LAMS-2674, Los Alamos Sci. Lab. p. 23.

18. Bittner H, Goretzki H (1962) Magnetische untersuchungen der carbide TiC, ZrC, HfC, VC, NbC und TaC, Monatsh Chem 93:1000-1004.

19. Norton JT, Lewis RK (1963) Properties of non-stoichiometric metallic carbides, Advanced Metals Research Corp, Somerville, Massachusetts, United States.

20. Rudy E, Bruckl C, Harmond DP (1965) Ternary phase equilibria in transition metal-boron-carbon-silicon systems. Air Force Materials Laboratory, Research and Technology Division.

21. Storms EK (1967) The refractory carbides. In: Refractory materials, a serie of monographs, vol. 2, New York, London: Academic Press.

22. Ramqvist L (1968) Variation of Lattice Parameter and Hardness with Carbon Content of Group 4 B Metal Carbides, Jka-Jernkontoret Ann 152:517.

23. Vicens J, Chermant JL (1972) Contribution to study of system Titanium-Carbon-Oxygen, Rev Chim Miner 9:557-567.

24. Kiparisov SS, Narva VK, Kolupaeva SY (1975) Effect of titanium carbide composition on the properties of titanium carbide-steel materials, Poroshk Metall 7:41–44.

25. Frage N, Levin L, Manor E et al (1996) Iron-titanium-carbon system. II. Microstructure of titanium carbide (TiCx) of various stoichiometries infiltrated with iron-carbon alloy, Scripta Mater 35:799-803.

26. Fernandes JC, Anjinho C, Amaral PM et al (2003) Characterisation of solar-synthesised TiCx (x=0.50, 0.625, 0.75, 0.85, 0.90 and 1.0) by X-ray diffraction, density and Vickers microhardness, Mater Chem Phys 77:711-718.

27. Hugosson HW, Korzhavyi P, Jansson U et al (2001) Phase stabilities and structural relaxations in substoichiometric TiC1-x, Phys Rev B 63:165116.

28. Andersson JO, Höglund L, Jönsson B, Ågren J (1990) Computer simulation of multicomponent diffusional transformations in steel. In: Purdy GR (ed) Fundamentals and applications of ternary diffusion. Pergamon Press, New York, pp 153-163.

29. Borgenstam A, Höglund L, Ågren J, Engström A (2000) DICTRA, a tool for simulation of diffusional transformations in alloys, J Phase Equilib 21:269-280.

30. Agren J (1990) Kinetics of Carbide Dissolution, Scand J Metall 19:2-8.

31. Gustafson Å (2000) Coarsening of TiC in austenitic stainless steel - experiments and simulations in comparison, Mat Sci Eng A-Struct 287:52-58.

32. Van Loo FJJ, Bastin GF (1989) On the diffusion of carbon in titanium carbide, Metall Trans A 20:403-411.